Addressing the pΩ femtoscopy correlation function using baryon-baryon effective potentials

6th Workshop on Future Directions in Spectroscopy Analysis

Marc Piquer i Méndez

Supervised by Juan Torres-Rincon and Assumpta Parreño

10th December 2025

UNIVERSITAT DE BARCELONA

ICCUB Institut de Ciències del Cosmos UNIVERSITAT DE BARCELONA

EXCELENCIA MARÍA DE MAEZTU 04/2025–03/2031

Femtoscopy correlation functions

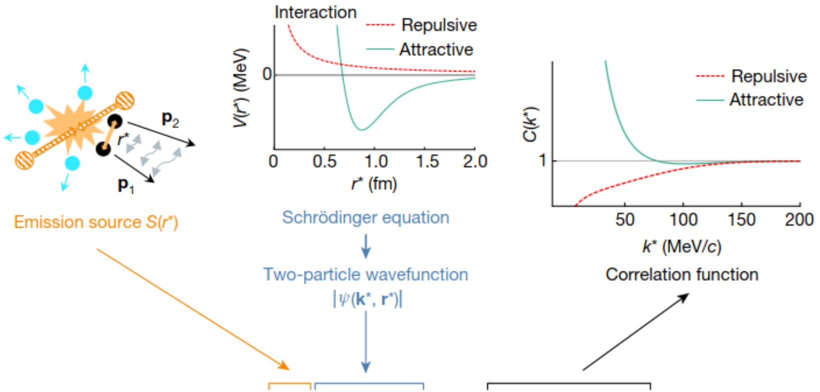

$$C(k^*) = \int S(r^*)\,|\psi(\mathbf{k}^*, \mathbf{r}^*)|^2\,d^3r^* = \xi(k^*)\,\frac{N_{\mathrm{same}}(k^*)}{N_{\mathrm{mixed}}(k^*)}$$

[ALI20] ALICE collaboration. *Nature* **588**: 232-238 (2020); [Koo77] S. E. Koonin. *Phys. Lett. B* **70**: 43-47 (1977).

Goal: ALICE results

The ALICE collaboration obtained results for the pΩ correlation function [ALI20].

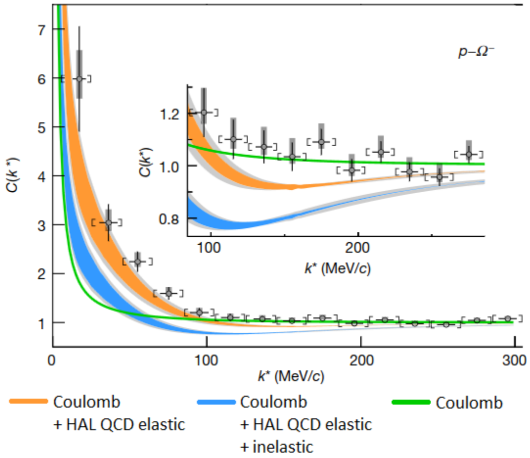

[IA+19] T. Iritani, S. Aoki et al. *Phys. Lett. B* **792**: 284-289 (2019).

Goal: ALICE results

The ALICE collaboration obtained results for the pΩ correlation function [ALI20].

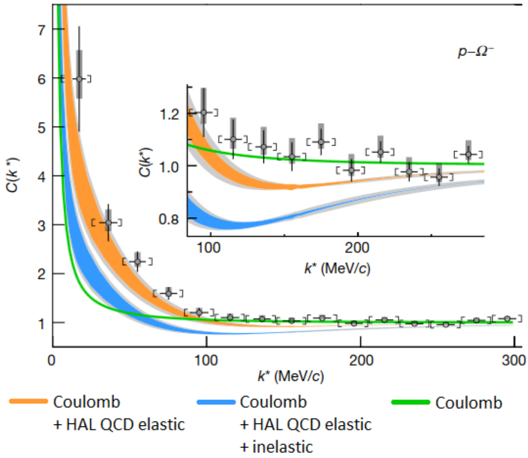

- There is no indication of a bound state in the experimental results.

[IA+19] T. Iritani, S. Aoki et al. *Phys. Lett. B* **792**: 284-289 (2019).

Goal: ALICE results

The ALICE collaboration obtained results for the pΩ correlation function [ALI20].

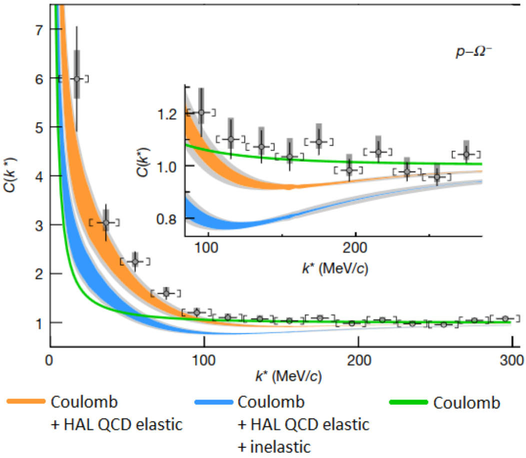

- There is no indication of a bound state in the experimental results.
- The orange band ($^5S_2$ channel) differs from the ALICE experimental results.

[IA+19] T. Iritani, S. Aoki et al. *Phys. Lett. B* **792**: 284-289 (2019).

Goal: ALICE results

The ALICE collaboration obtained results for the pΩ correlation function [ALI20].

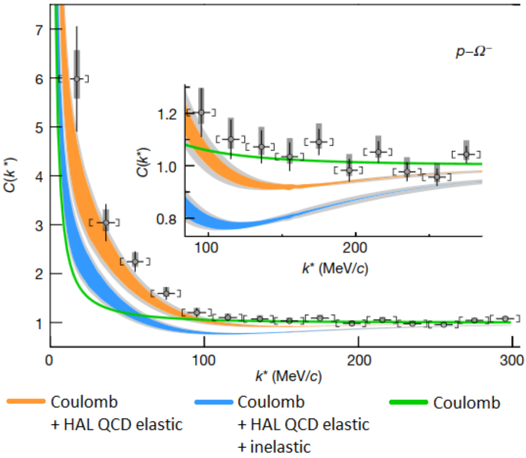

- There is no indication of a bound state in the experimental results.
- The orange band ($^5S_2$ channel) differs from the ALICE experimental results.
- Adding the $^3S_1$ channel could improve the agreement.

[IA+19] T. Iritani, S. Aoki et al. *Phys. Lett. B* **792**: 284-289 (2019).

Method: numerical solution of the Schrödinger equation and effective potentials

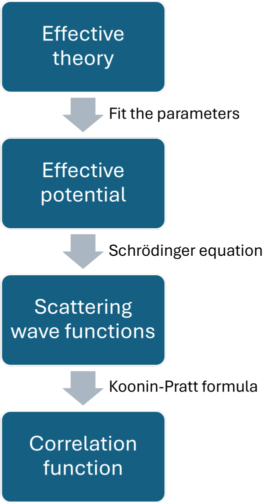

Method: numerical solution of the Schrödinger equation and effective potentials

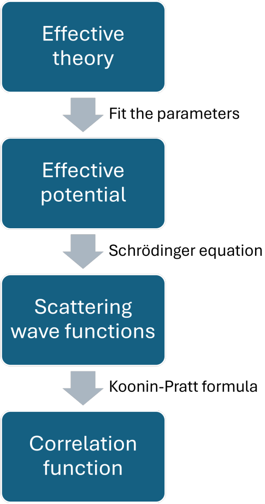

To compute the femtoscopy correlation function we need the scattering wave functions and a potential to compute them.

Method: numerical solution of the Schrödinger equation and effective potentials

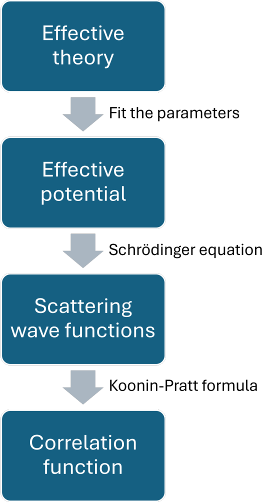

To compute the femtoscopy correlation function we need the scattering wave functions and a potential to compute them.

We will build the potential using an effective theory at leading order (LO).

Method: numerical solution of the Schrödinger equation and effective potentials

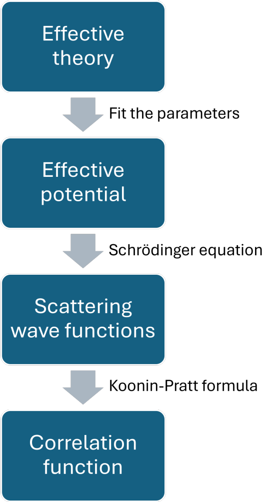

To compute the femtoscopy correlation function we need the scattering wave functions and a potential to compute them.

We will build the potential using an effective theory at leading order (LO).

For each wave number k (at the center of mass reference frame) we solve the Schrödinger equation numerically and obtain the scattering wave functions.

Method: numerical solution of the Schrödinger equation and effective potentials

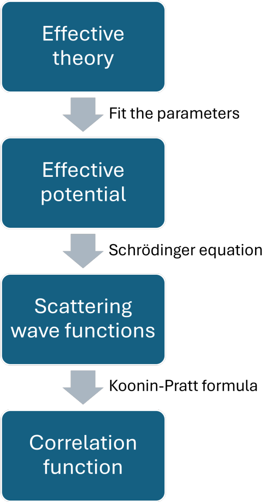

To compute the femtoscopy correlation function we need the scattering wave functions and a potential to compute them.

We will build the potential using an effective theory at leading order (LO).

For each wave number k (at the center of mass reference frame) we solve the Schrödinger equation numerically and obtain the scattering wave functions.

We then integrate and obtain the correlation functions through the Koonin-Pratt formula.

LO effective potential diagrams

To obtain the contributing diagrams, we use Weinberg's power counting,

$$\nu = 2 + 2L - B + \sum_i V_i(d_i + b_i/2 - 2). \tag{1}$$

LO effective potential diagrams

To obtain the contributing diagrams, we use Weinberg's power counting,

$$\nu = 2 + 2L - B + \sum_i V_i(d_i + b_i/2 - 2). \tag{1}$$

Thus, at LO ($\nu = 0$), we have contact terms ($b_i = 4,\ d_i = 0$) or one-meson exchanges ($b_i = 2,\ d_i = 1$).

LO effective potential diagrams

To obtain the contributing diagrams, we use Weinberg's power counting,

$$\nu = 2 + 2L - B + \sum_i V_i(d_i + b_i/2 - 2). \quad (1)$$

Thus, at LO ($\nu = 0$), we have contact terms ($b_i = 4$, $d_i = 0$) or one-meson exchanges ($b_i = 2$, $d_i = 1$).

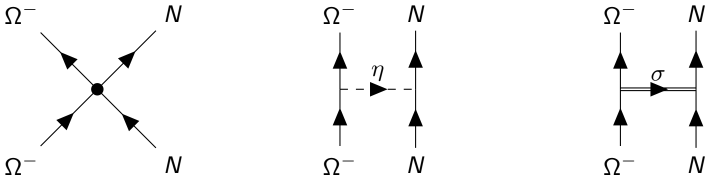

Figure 1: Diagrams considered for the elastic channels.

LO potential expression

For the nucleon vertices, we use the Lagrangian

$$\mathcal{L}_{\mathrm{O}} = \mathrm{tr}[\bar{B}(\mathrm{i}\gamma^{\mu}\nabla_{\mu} - m_B)B] + D\,\mathrm{tr}[\bar{B}\gamma^{\mu}\gamma_5\{u_{\mu}, B\}] + F\,\mathrm{tr}[\bar{B}\gamma^{\mu}\gamma_5[u_{\mu}, B]]. \qquad (2)$$

[3] E. Jenkins and A. V. Manohar. "Chiral corrections to the baryon axial currents". *Phys. Lett. B* **259**: 353-358 (1991).

LO potential expression

For the nucleon vertices, we use the Lagrangian

$$\mathcal{L}_{\mathrm{O}} = \mathrm{tr}[\bar{B}(\mathrm{i}\gamma^{\mu}\nabla_{\mu} - m_B)B] + D\,\mathrm{tr}[\bar{B}\gamma^{\mu}\gamma_5\{u_{\mu}, B\}] + F\,\mathrm{tr}[\bar{B}\gamma^{\mu}\gamma_5[u_{\mu}, B]]. \qquad (2)$$

Whereas for the Ω vertices, we use[3]

$$\mathcal{L}_{\mathrm{D}} = -\mathrm{i}\,\bar{T}^{\mu}(v\cdot\nabla)T_{\mu} + \Delta m\,\bar{T}^{\mu}T_{\mu} + 2\mathcal{H}\,\bar{T}^{\mu}\hat{\mathbb{S}}_{\nu}u^{\nu}T_{\mu}. \qquad (3)$$

[3] E. Jenkins and A. V. Manohar. "Chiral corrections to the baryon axial currents". *Phys. Lett. B* **259**: 353-358 (1991).

LO potential expression

For the nucleon vertices, we use the Lagrangian

$$\mathcal{L}_{\rm O} = {\rm tr}[\bar{B}({\rm i}\gamma^{\mu}\nabla_{\mu} - m_B)B] + D\,{\rm tr}[\bar{B}\gamma^{\mu}\gamma_5\{u_{\mu}, B\}] + F\,{\rm tr}[\bar{B}\gamma^{\mu}\gamma_5[u_{\mu}, B]]. \quad (2)$$

Whereas for the Ω vertices, we use[3]

$$\mathcal{L}_{\rm D} = -{\rm i}\bar{T}^{\mu}(v\cdot\nabla)T_{\mu} + \Delta m\bar{T}^{\mu}T_{\mu} + 2\mathcal{H}\bar{T}^{\mu}\hat{\mathbb{S}}_{\nu}u^{\nu}T_{\mu}. \quad (3)$$

This way, we obtain the three contribuctons for the elastic channels, $^5S_2$ and $^3S_1$:

$$\begin{aligned}
\hat{V}_{\rm ct}(\vec{r}) =& (C_0^0 + C_0^1\vec{\mathbb{S}}\cdot\vec{\sigma})f_\delta(r),\\
\hat{V}_{\eta}(\vec{r}) =& C_{N\eta\bar{N}}C_{\Omega\eta\bar{\Omega}}\frac{{m_\eta}^2}{3}\left(\frac{{\Lambda_\eta}^2}{{\Lambda_\eta}^2 - {m_\eta}^2}\right)^2\\
&\left[\frac{e^{-m_\eta r}}{4\pi r} - \frac{e^{-\Lambda_\eta r}}{4\pi r} + \frac{({m_\eta}^2 - {\Lambda_\eta}^2)\Lambda_\eta}{8\pi {m_\eta}^2}e^{-\Lambda_\eta r}\right]\vec{\mathbb{S}}\cdot\vec{\sigma},\\
\hat{V}_{\sigma}(\vec{r}) =& -C_{N\sigma\bar{N}}C_{\Omega\sigma\bar{\Omega}}\left(\frac{{\Lambda_\sigma}^2}{{\Lambda_\sigma}^2 - {m_\eta}^2}\right)^2\left[\frac{e^{-m_\sigma r}}{4\pi r} - \frac{e^{-\Lambda_\sigma r}}{4\pi r} + \frac{{m_\sigma}^2 - {\Lambda_\sigma}^2}{8\pi\Lambda_\sigma}e^{-\Lambda_\sigma r}\right].
\end{aligned} \quad (4)$$

[3] E. Jenkins and A. V. Manohar. "Chiral corrections to the baryon axial currents". *Phys. Lett. B* **259**: 353-358 (1991).

Potential parametrizations

We parametrize the potential by either fitting the $^5S_2$ channel to the HAL QCD potential or by choosing *a priori* reasonable values for the parameters.

[Flo14] M. Florit Gual. Master's thesis, Universitat de Barcelona, 2014; [Mac85] R. Machleidt in *Relativistic dynamics and Quark-Nuclear Physics: Proc. Los Alamos Workshop* (Wiley, New York, 1986).

Potential parametrizations

We parametrize the potential by either fitting the $^5S_2$ channel to the HAL QCD potential or by choosing *a priori* reasonable values for the parameters.

	C_0^0(MeV^{-2})	C_0^1(MeV^{-2})	$C_{\Omega\sigma\bar{\Omega}}$	Λ_η(MeV)	Λ_σ(MeV)
Florit	$5.00 \cdot 10^{-3}$	$1.00 \cdot 10^{-3}$			
Reduced Florit	$1.25 \cdot 10^{-3}$	$0.25 \cdot 10^{-3}$			
No FF	$-8.06(6) \cdot 10^{-6}$	$-1.61(2) \cdot 10^{-6}$	0.8858(2)		
Fixed FF	$1.133(5) \cdot 10^{-5}$	$2.267(9) \cdot 10^{-6}$	1.882(8)	900	1200
Free FF	$6.59(6) \cdot 10^{-6}$	$1.32(2) \cdot 10^{-6}$	2.58(3)	917.4(7)	622(6)

[Flo14] M. Florit Gual. Master's thesis, Universitat de Barcelona, 2014; [Mac85] R. Machleidt in *Relativistic dynamics and Quark-Nuclear Physics: Proc. Los Alamos Workshop* (Wiley, New York, 1986).

Potential parametrizations

We parametrize the potential by either fitting the $^5S_2$ channel to the HAL QCD potential or by choosing *a priori* reasonable values for the parameters.

	C_0^0(MeV^{-2})	C_0^1(MeV^{-2})	$C_{\Omega\sigma\bar{\Omega}}$	Λ_η(MeV)	Λ_σ(MeV)
Florit	$5.00 \cdot 10^{-3}$	$1.00 \cdot 10^{-3}$			
Reduced Florit	$1.25 \cdot 10^{-3}$	$0.25 \cdot 10^{-3}$			
No FF	$-8.06(6) \cdot 10^{-6}$	$-1.61(2) \cdot 10^{-6}$	0.8858(2)		
Fixed FF	$1.133(5) \cdot 10^{-5}$	$2.267(9) \cdot 10^{-6}$	1.882(8)	900	1200
Free FF	$6.59(6) \cdot 10^{-6}$	$1.32(2) \cdot 10^{-6}$	2.58(3)	917.4(7)	622(6)

[Flo14] M. Florit Gual. Master's thesis, Universitat de Barcelona, 2014; [Mac85] R. Machleidt in *Relativistic dynamics and Quark-Nuclear Physics: Proc. Los Alamos Workshop* (Wiley, New York, 1986).

Results: $^5S_2$ channel (repulsive)

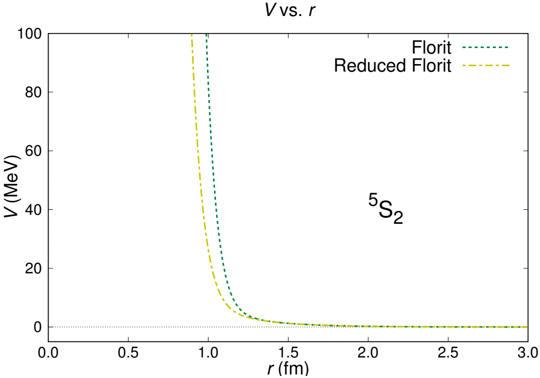

Results: $^5S_2$ channel (repulsive)

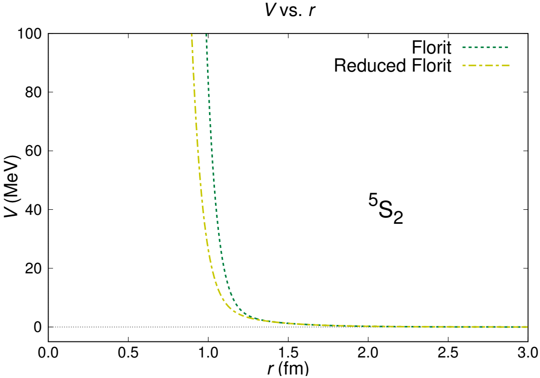

- The Florit parametrizations yield very repulsive potentials.

Results: $^5S_2$ channel (repulsive)

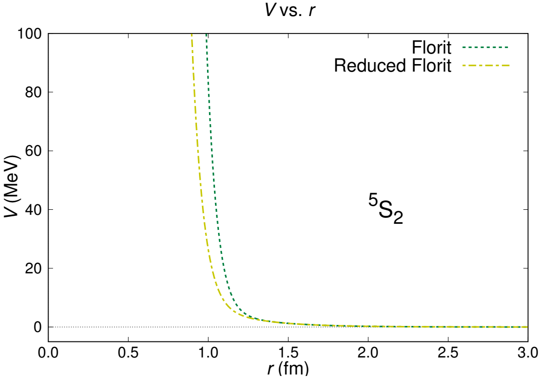

- The Florit parametrizations yield very repulsive potentials.
- This differs strongly from the HAL QCD potential, as well as the correlation function behaviour.

Results: $^5S_2$ channel (attractive)

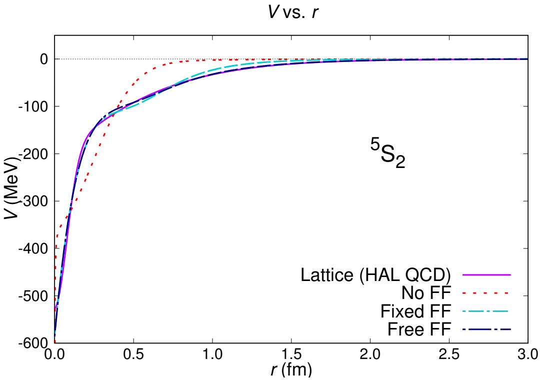

Results: $^5S_2$ channel (attractive)

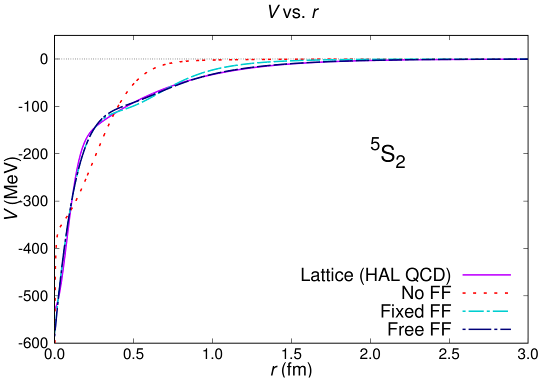

- The free FF fit reproduces the lattice results quite faithfully.

Results: $^5S_2$ channel (attractive)

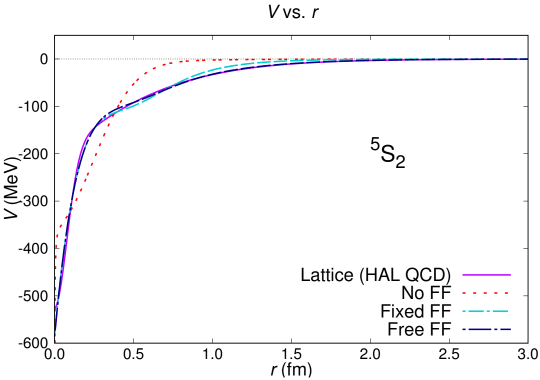

- The free FF fit reproduces the lattice results quite faithfully.
- The fixed FF is also a reasonable fit, apparently.

Results: $^5S_2$ channel (attractive)

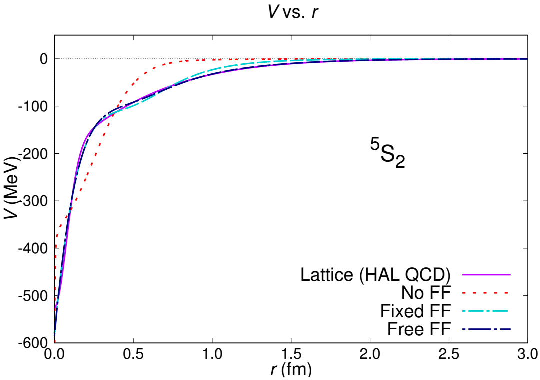

- The free FF fit reproduces the lattice results quite faithfully.
- The fixed FF is also a reasonable fit, apparently.
- The no FF fit does not reproduce well the lattice results at all. We will disregard it.

Results: $^5S_2$ channel (attractive)

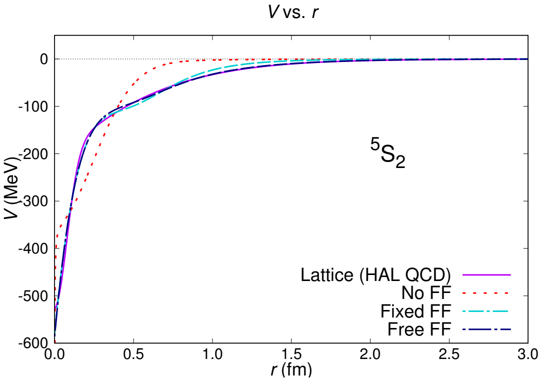

- The free FF fit reproduces the lattice results quite faithfully.
- The fixed FF is also a reasonable fit, apparently.
- The no FF fit does not reproduce well the lattice results at all. We will disregard it.
- The fixed FF and free FF fits admit bound states.

Results: $^5S_2$ channel (attractive)

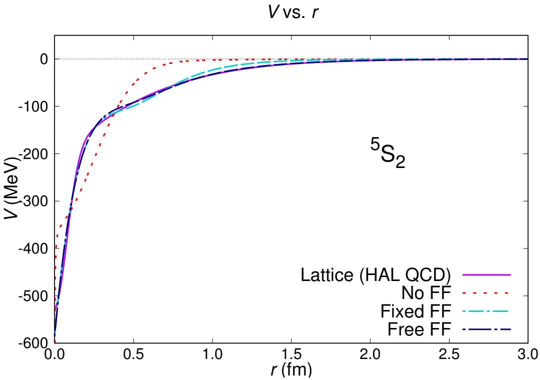

- The free FF fit reproduces the lattice results quite faithfully.
- The fixed FF is also a reasonable fit, apparently.
- The no FF fit does not reproduce well the lattice results at all. We will disregard it.
- The fixed FF and free FF fits admit bound states.
- The free FF one is found at -2.20 MeV.

Results: $^3S_1$ channel

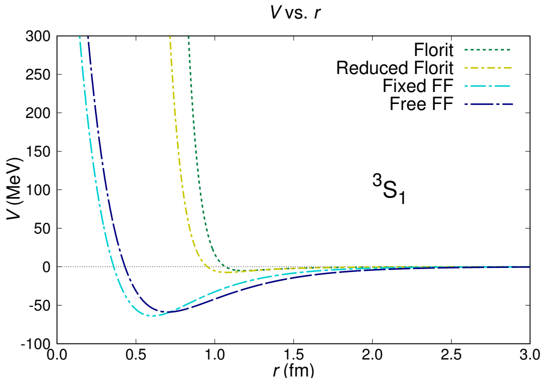

Results: $^3S_1$ channel

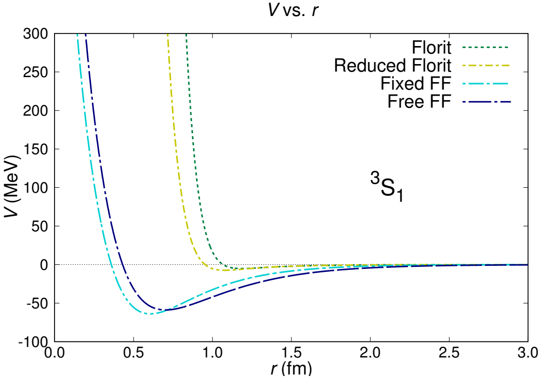

- All of the $^3S_1$ potentials show a minimum.

Results: $^3S_1$ channel

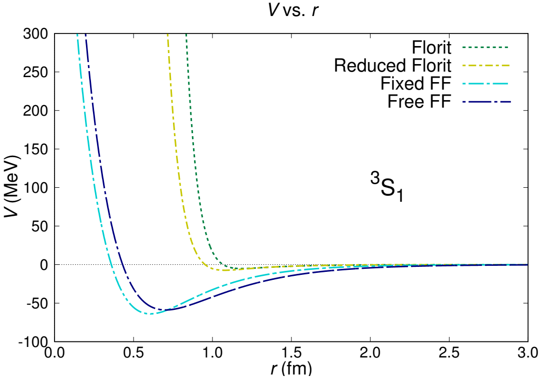

- All of the $^3S_1$ potentials show a minimum.
- Only the fit potentials admit a bound state.

Results: $^3S_1$ channel

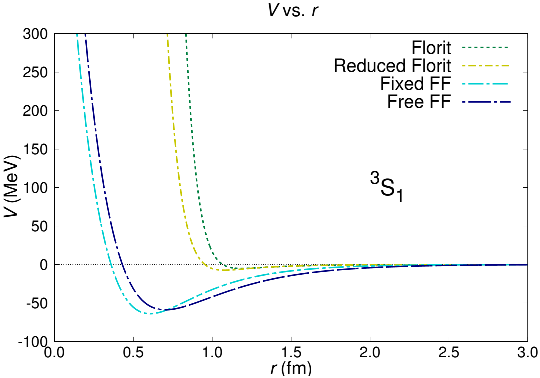

- All of the $^3S_1$ potentials show a minimum.
- Only the fit potentials admit a bound state.
- For the free FF potential, it is found at -0.481 MeV.

Correlation function generalities

With the potential, we can get the wave functions for each k, with which we can compute the correlation function.

Correlation function generalities

With the potential, we can get the wave functions for each k, with which we can compute the correlation function.

Approximation: the interaction only affects the s mode. Then, without the Coulomb interaction,

$$C(k) = 1 + 4\pi \int_0^{\infty} S(r) \left[|u_0(r,k)|^2 - (r j_0(kr))^2 \right] \mathrm{d}r, \tag{5}$$

Correlation function generalities

With the potential, we can get the wave functions for each k, with which we can compute the correlation function.

Approximation: the interaction only affects the s mode. Then, without the Coulomb interaction,

$$C(k) = 1 + 4\pi \int_0^\infty S(r) \left[|u_0(r,k)|^2 - (rj_0(kr))^2 \right] \mathrm{d}r, \tag{5}$$

whereas with Coulomb interaction

$$\begin{aligned} C(k) =& 2\pi e^{-\pi\gamma} |\Gamma(1+\mathrm{i}\gamma)|^2 \int_{-1}^{1} \mathrm{d}\cos\theta \int_0^\infty r^2 S(r) |{}_1F_1(-\mathrm{i}\gamma; 1; \mathrm{i}kr(1-\cos\theta))|^2 \,\mathrm{d}r \\ &+ 4\pi \int_0^\infty S(r) \left[|u_0(r,k)|^2 - |F_0(k,r)/k|^2 \right] \mathrm{d}r \,. \end{aligned} \tag{6}$$

Correlation function generalities

With the potential, we can get the wave functions for each k, with which we can compute the correlation function.

Approximation: the interaction only affects the s mode. Then, without the Coulomb interaction,

$$C(k) = 1 + 4\pi \int_0^\infty S(r) \left[|u_0(r,k)|^2 - (r j_0(kr))^2 \right] \mathrm{d}r, \tag{5}$$

whereas with Coulomb interaction

$$\begin{aligned} C(k) =& 2\pi e^{-\pi\gamma} |\Gamma(1+\mathrm{i}\gamma)|^2 \int_{-1}^{1} \mathrm{d}\cos\theta \int_0^\infty r^2 S(r) |{}_1F_1(-\mathrm{i}\gamma; 1; \mathrm{i}kr(1-\cos\theta))|^2 \,\mathrm{d}r \\ &+ 4\pi \int_0^\infty S(r) \left[|u_0(r,k)|^2 - |F_0(k,r)/k|^2 \right] \mathrm{d}r \,. \end{aligned} \tag{6}$$

Following the original ALICE article, we use a Gaussian source with radius 0.95 fm.

Correlation function generalities

With the potential, we can get the wave functions for each k, with which we can compute the correlation function.

Approximation: the interaction only affects the s mode. Then, without the Coulomb interaction,

$$C(k) = 1 + 4\pi \int_0^\infty S(r) \left[|u_0(r,k)|^2 - (r j_0(kr))^2 \right] \mathrm{d}r, \quad (5)$$

whereas with Coulomb interaction

$$\begin{aligned} C(k) =& 2\pi e^{-\pi\gamma} |\Gamma(1+\mathrm{i}\gamma)|^2 \int_{-1}^{1} \mathrm{d}\cos\theta \int_0^\infty r^2 S(r) |{}_1F_1(-\mathrm{i}\gamma; 1; \mathrm{i}kr(1-\cos\theta))|^2 \, \mathrm{d}r \\ &+ 4\pi \int_0^\infty S(r) \left[|u_0(r,k)|^2 - |F_0(k,r)/k|^2 \right] \mathrm{d}r \,. \end{aligned} \quad (6)$$

Following the original ALICE article, we use a Gaussian source with radius 0.95 fm. We have two channels. We will, then, perform a spin-weighted average

$$C(k) = \frac{3 C_{^3S_1}(k) + 5 C_{^5S_2}(k)}{8}. \quad (7)$$

Results: pΩ correlation function

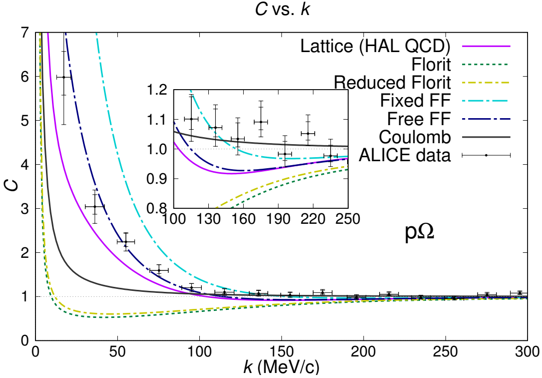

Results: pΩ correlation function

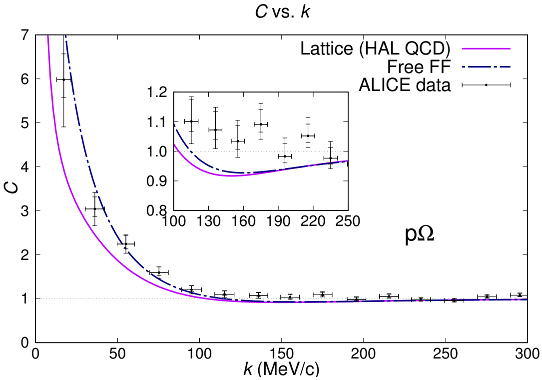

- We see that adding the $^3S_1$ channel does improve on the results obtained by the lattice HAL QCD potential.

Results: pΩ correlation function

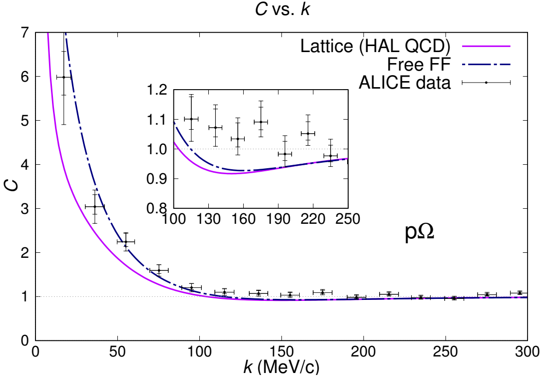

- We see that adding the $^3S_1$ channel does improve on the results obtained by the lattice HAL QCD potential.
- There is even some room left for the inelastic channels to provide a non-negligible contribution.

ML outlook

Another approach would be to try to obtain the potential parameters from the correlation function values.

ML outlook

Another approach would be to try to obtain the potential parameters from the correlation function values.

We can approximate them by using a neural network trained with our model.

ML outlook

Another approach would be to try to obtain the potential parameters from the correlation function values.

We can approximate them by using a neural network trained with our model.

Work is still in progress. We only have some preliminary results, for a PyTorch NN with LR = 0.005 and ADAM optimizer.

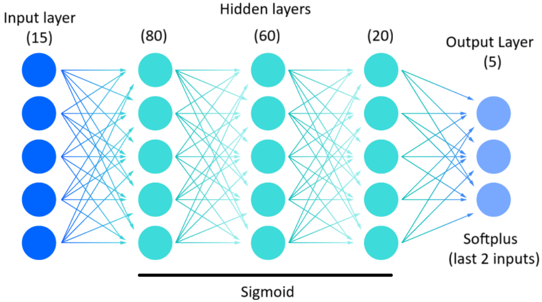

Preliminary ML results

$^5S_2$ channel

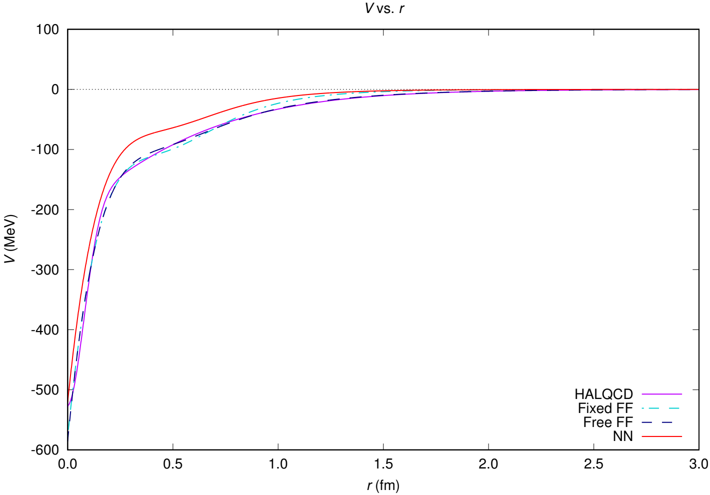

Preliminary ML results

$^3S_1$ channel

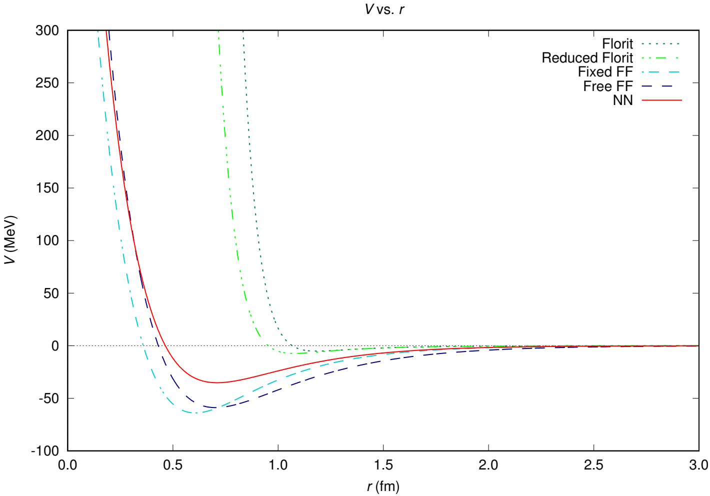

Preliminary ML results

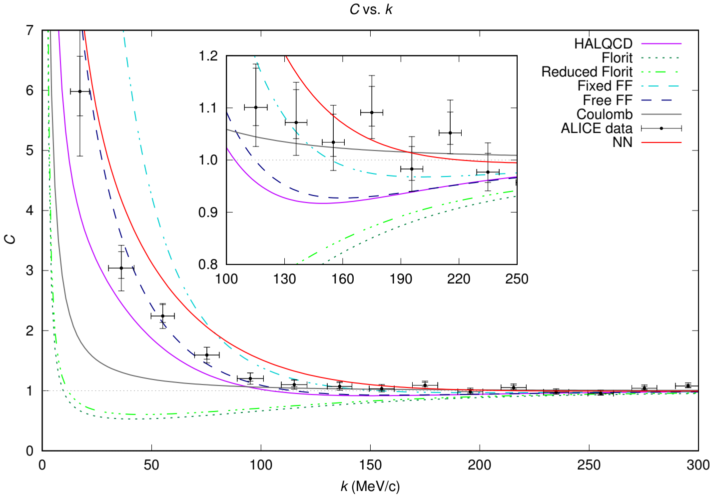

Summary and conclusions

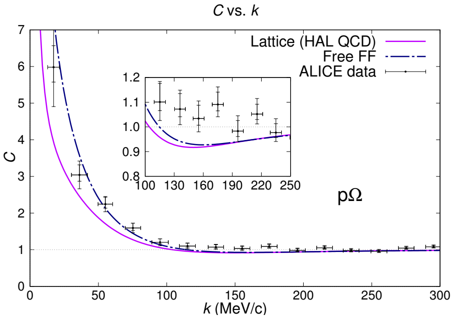

Summary and conclusions

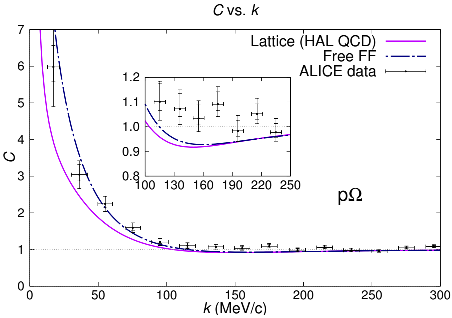

- We have developed an effective potential, fitting the $^5S_2$ elastic channel, which gives the $^3S_1$ elastic channel.

Summary and conclusions

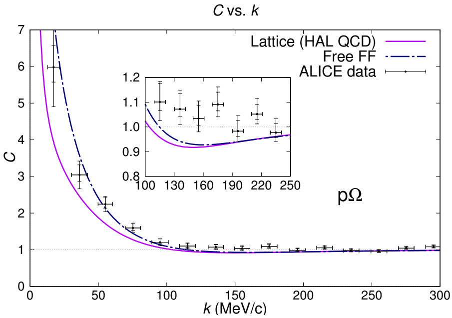

- We have developed an effective potential, fitting the $^5S_2$ elastic channel, which gives the $^3S_1$ elastic channel.
- We have obtained bound states for both elastic channels.

Summary and conclusions

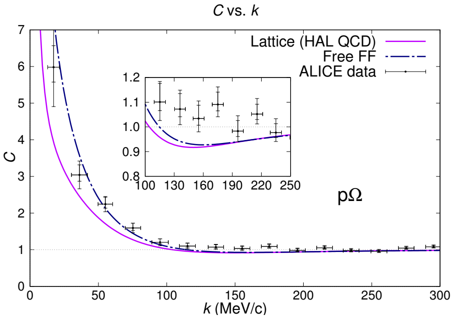

- We have developed an effective potential, fitting the $^5S_2$ elastic channel, which gives the $^3S_1$ elastic channel.
- We have obtained bound states for both elastic channels.
- We have computed the scattering wave functions and, with them, the pΩ femtoscopy correlation functions.

Summary and conclusions

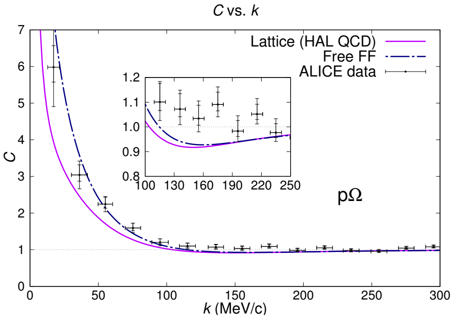

- We have developed an effective potential, fitting the ${}^5S_2$ elastic channel, which gives the ${}^3S_1$ elastic channel.
- We have obtained bound states for both elastic channels.
- We have computed the scattering wave functions and, with them, the pΩ femtoscopy correlation functions.
- Since the higher partial waves will contribute positively to C, we see that the inelastic channels may provide a negative contribution.

Outlook

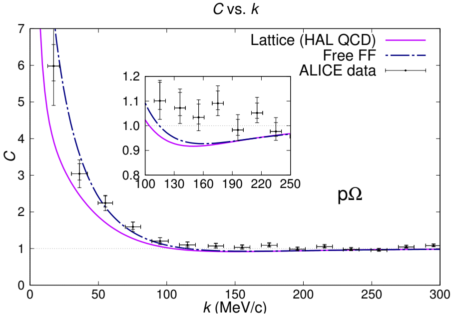
C vs. k
Lattice (HAL QCD)
Free FF
ALICE data
pΩ
C
k (MeV/c)
0
1
2
3
4
5
6
7
50
100
150
200
250
300
1.2
1.1
1.0
0.9
0.8
130
160
190
220

Outlook

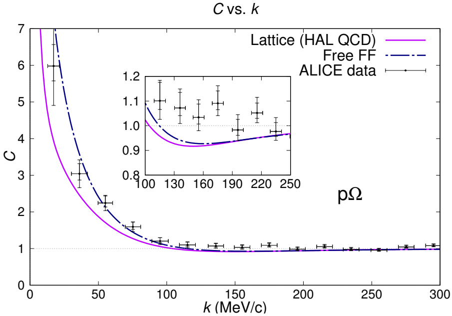

Future work:

Outlook

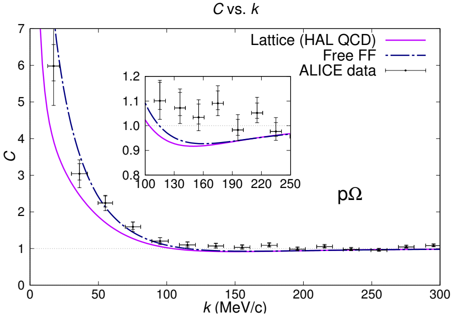

Future work:

- Include the higher partial waves and inelastic channels.

Outlook

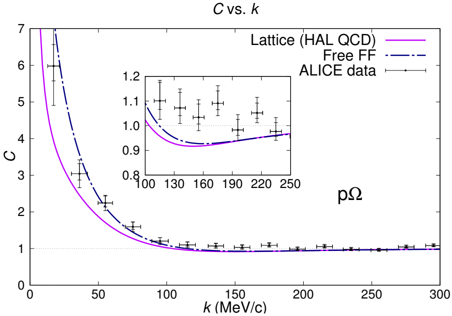

Future work:

- Include the higher partial waves and inelastic channels.
- Study the dependence on the source function.

Outlook

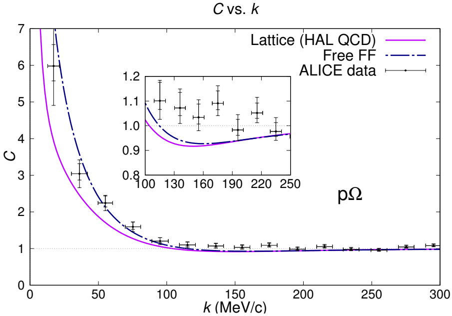

Future work:

- Include the higher partial waves and inelastic channels.
- Study the dependence on the source function.
- Use this method to study other systems (pΞ, ΩΩ. . .).

Outlook

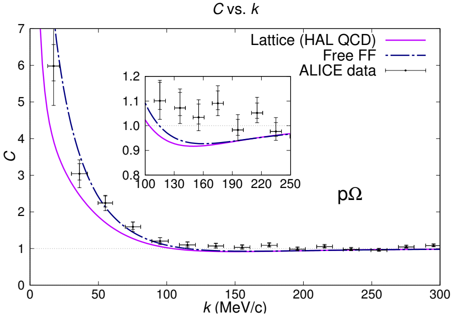

Future work:

- Include the higher partial waves and inelastic channels.
- Study the dependence on the source function.
- Use this method to study other systems (pΞ, ΩΩ. . .).
- Keep working on the neural network technique.

Thank you for your attention!

Results: $^5S_2$ bound states

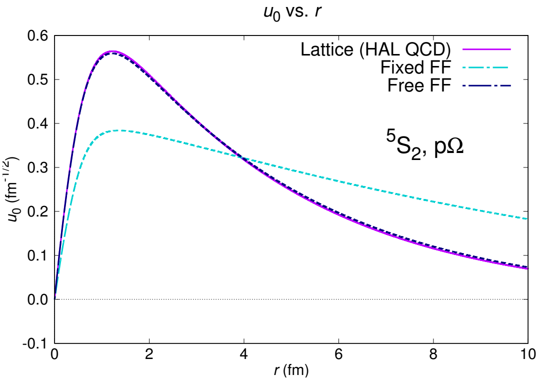

- The HAL QCD potential and the good fits yield bound states.
- The proximity between the free FF fit and lattice shows that the free FF fit is the better fit.
- Said bound state appears about $E \sim -2.2$ MeV.

Results: $^3S_1$ bound states

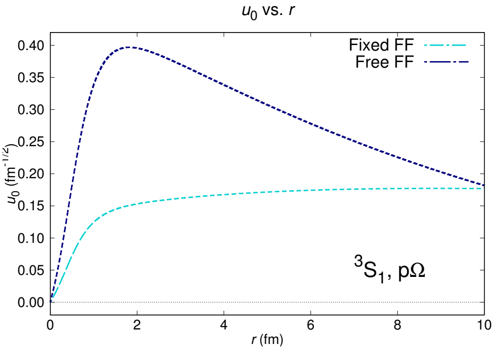

- With the added Coulomb interaction, both fits admit $^3S_1$ bound states.
- The free FF fit one is about $E \sim -4.81 \cdot 10^{-1}$ MeV.

Results: $^5S_2$ pΩ scattering wave functions

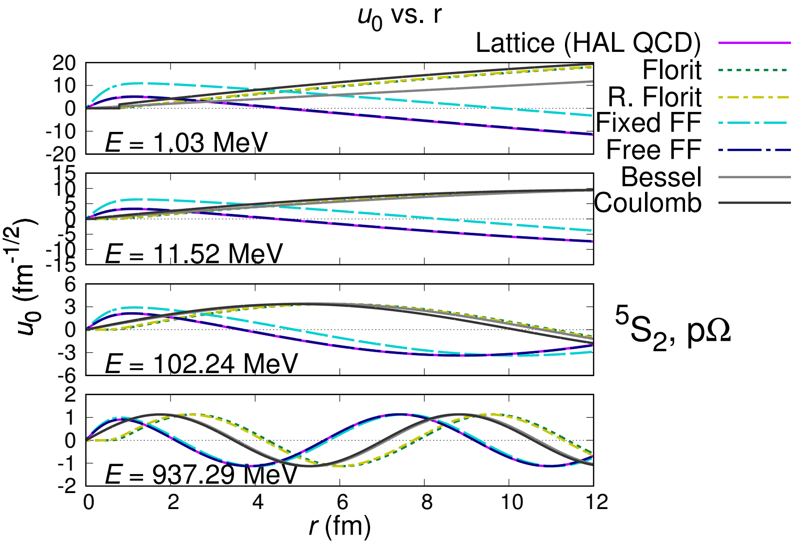

Results: $^{3}S_{1}$ pΩ scattering wave functions